IOP Conf. Series: Materials Science and Engineering **374** (2018) 012021 doi:10.1088/1757-899X/374/1/012021

Magnetic Properties of Rapid Cooled FeCoB Based Alloys Produced by Injection Molding

M Nabialek[1*], B Jeż[1], K Jeż[1], P Pietrusiewicz[1], K Gruszka[1], K Błoch[1], J Gondro[1], J Rządki[1], M M A B Abdullah[2], A V Sandu[3] and M Szota[4]

1 Institute of Physics, Faculty of Production Engineering and Materials Technology, Czestochowa University of Technology, 19 Armii Krajowej Str., 42-200 Czestochowa, Poland

2 Gheorghe Asachi Technical University of Iasi, Faculty of Materials Science and Engineering, 41 D. Mangeron Blvd., 70050, Iasi, Romania

3 Geopolymer & Green Technology (CeGeoGTech), School of Material Engineering, Universiti Malaysia Perlis (UniMAP), 01000 Kangar, Perlis Malaysia

4 Institute of Materials Engineering, Faculty of Production Engineering and Materials Technology, Czestochowa University of Technology, 19 Armii Krajowej Str., 42-200 Czestochowa, Poland

E-mail: nmarcell@wp.pl

Abstract. The paper presents the results of investigations of the structure and magnetic properties of massive rapid cooled $Fe_{50-x}Co_{20+x}B_{20}Cu_1Nb_9$ alloys (where x = 0, 5). Massive alloys were made using the method of injecting a liquid alloy into a copper mold. Samples were obtained in the form of 0.5 mm thick plates. The structure of the obtained samples was examined using an X-ray diffractometer equipped with a CuKα lamp. The phase composition of the alloys formed was determined using the Match program. By using Sherrer's dependence the grain sizes of the identified crystalline phases were estimated. Using the Faraday magnetic balance, the magnetization of samples as a function of temperature in the range from room temperature to 850K was measured. Magnetization of saturation and value of the coercive field for the prepared alloys were determined on the basis of magnetic hysteresis loop measurement using the LakeShore vibration magnetometer.

1. Introduction

Amorphous materials are a relatively new group of functional materials, known for over 60 years. Originally, materials with amorphous structure were produced in the form of thin strips and layers [1]. Quick cooling of the liquid alloy allowed to block the crystallization process. In this way, it is possible to maintain a chaotic arrangement of atoms in the volume of material. This configuration of atoms is suitable for liquids. Amorphous materials combine the properties of solids and liquid phases, which implies their extraordinary properties. Taking the form of a solid with a liquid structure, amorphous alloys show better properties compared to their crystalline counterparts [2-6].

However, amorphous alloys produced in the form of thin strips have considerably limited applicability. Few μm for many years was the maximum thickness of this type of materials. Thickness of amorphous strips reaching several dozen μm. Numerous studies of scientists from around the world and, above all, the works of A. Inoue have contributed to the emergence of a new group of materials,

massive amorphous materials. Three empirical principles formulated by a Japanese scientist are some kind of guidelines for the production of amorphous materials [7, 8]. The multi-componentity of the alloy, the negative heat of mixing of the components and the correspondingly large differences in the length; of the atomic diameters of the main components allow the inhibition of the crystallization process during the cooling of the liquid alloy. Atoms of individual components can be treated as spheres with different atomic radii. Appropriate differences in their radii cause their mutual blocking during diffusion processes occurring during solidification of the liquid melt. The negative heat of mixing< influences the increase in the viscosity of the alloy, which additionally hinders the migration of atoms. Preventing the movement of atoms significantly slows down the crystallization process. Cooling of the alloy at a suitable rate allows solidification of the alloy in the configuration of atoms suitable for liquids. Obtaining volumetric amorphous alloys is possible during cooling at a speed of 10^0 - 10^3 K / s. Well-known methods for producing massive amorphous materials are suction and injection methods. Using these methods, one can create a rapid-cooled alloy in the form of cores, rods or plates.

Amorphous alloys are often heat treated to obtain a nanocrystalline structure. Materials of this type are often characterized by better properties than their amorphous precursor. Depending on the chemical composition used, it is possible to manufacture partially crystallized alloys in a one-stage process as soon as it solidifies [9, 10]. The selection of the appropriate chemical composition and cooling rate allows to slow the crystallization process in a way that allows only a certain amount of crystal phase grains to be distributed in the amorphous matrix.

Amorphous and nanocrystalline materials are particularly interesting group of materials due to their good magnetic properties. Alloys with high content of iron and cobalt are characterized by the so-called magnetically soft properties, characterized by among others: high saturation magnetization and low coercive field [11-18]. In addition, alloys with a high cobalt content of ten have a high Curie temperature.

The purpose of the work was to produce volumetric two-phase rapid cooled alloys with chemical composition $Fe_{50-x}Co_{20+x}B_{20}Cu_1Nb_9$ (gdzie x = 0, 5) and to study their structure and magnetic properties.

2. Methods and material

The base alloy with the chemical composition $Fe_{50-x}Co_{20+x}B_{20}Cu_1Nb_9$ (where x = 0, 5) was made using a plasma furnace. For this purpose, the alloy components were measured to within 0.001 grams. Five gram weight was allocated to the polycrystalline ingot. Chemical elements with high purity, over 99.99%, were used. The ingot was made in an arc furnace under a protective atmosphere of argon. The temperature of the plasma arc was regulated by the intensity of the current flowing through the electrode. Before the actual melting of the batch, pure titanium was melted which has a significant impact on the purity of the atmosphere in the working chamber. The batch was melted several times, each time turning the ingot over to the other side using a manipulator, which ensures better mixing of the alloy components. Purified from external contamination of ingots, crushed into smaller pieces.

The ingot served as a batch material to produce a rapid cooled alloy by the method of injecting a liquid alloy into a copper mold. The alloys were produced in the form of 5mm x 5mm x 0.5mm tiles. Pieces of a polycrystalline ingot were placed in a quartz capillary. The batch was inductively melted at a constant current. The liquid alloy was forced into the copper mold through a hole in a 1mm diameter quartz capillary. During the process, constant argon pressure was maintained. The entire casting process of the high-temperature melt was carried out under a protective gas (argon) after reaching a vacuum in the working chamber (10-5 mbar.) To obtain a clean atmosphere, the working chamber and the injection system were subjected to additional argon washing. The liquid melt was then injected into copper water cooled molds with a hollow core in the shape of a cylinder The scheme for the production of rapid cooled alloys is shown in Figure 1.

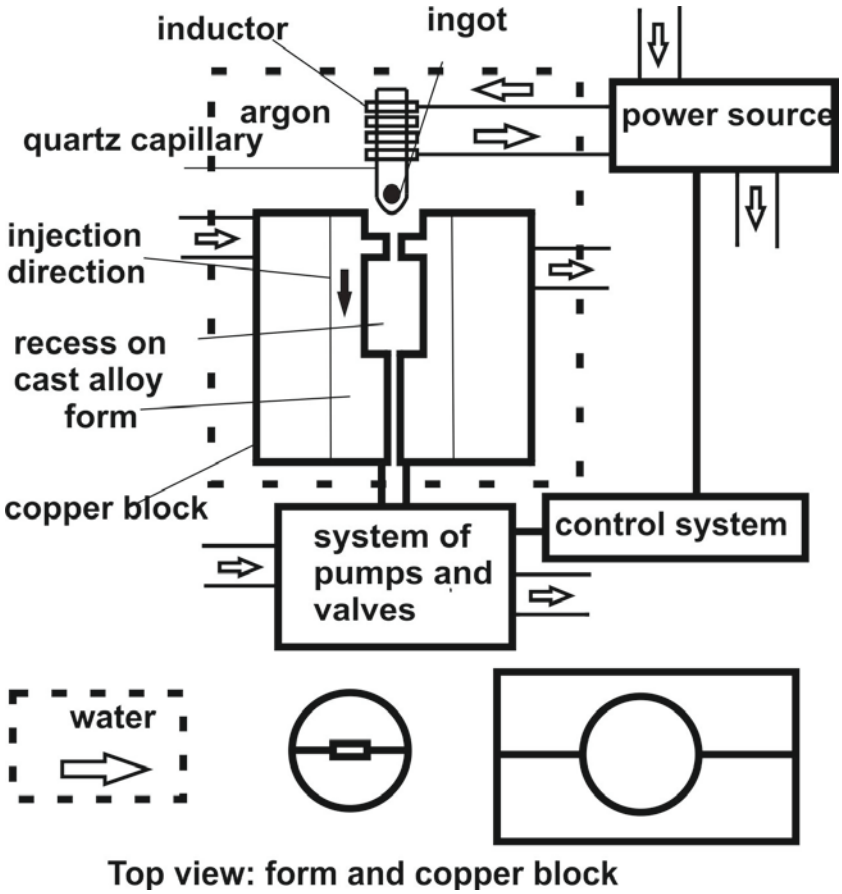

Figure 1. Scheme of the system for the production of rapid cooled alloys by the injection method.

The presented method of producing quick-cooled alloys allows the production of bar materials. The structure of the produced $Fe_{50-x}Co_{20+x}B_{20}Cu_1Nb_9$ alloy samples (where x = 0.5) was investigated using X-ray diffraction (Brucker apparatus, Cu-Kα lamp). Advance 8 model. The thermomagnetic properties of the produced samples were examined by Faraday's magnetic weight. The size of crystallites formed during the alloying process was estimated using the Sherrer formula (1):

$$D=(\lambda*K)/2\beta_0 cos\Theta \quad (1)$$

K –Scherrer shape coefficient (K = 0,91),
λ – characteristic radiation wavelength,
B_0 – half-width intensity (background was included In analysis),
Θ – Bragg angle.

3. Results

Figure 2 shows diffraction patterns for $Fe_{50-x}Co_{20+x}B_{20}Cu_1Nb_9$ in as cast state.

The investigations were carried out in the 2 theta angle range from 30° to 100°. On recorded diffractograms, narrow peaks of considerable intensity can be distinguished from crystalline phases: Fe_2B, BCo and αFe. In the samples, there is one more crystalline phase that could not be identified. In addition, the wide maximum in the angle of 2 theta from 40° to 50° is visible on the diffractograms. The maximum called the amorphous halo is derived from X-rays scattered on chaotically distributed atoms in the volume of the alloy samples.

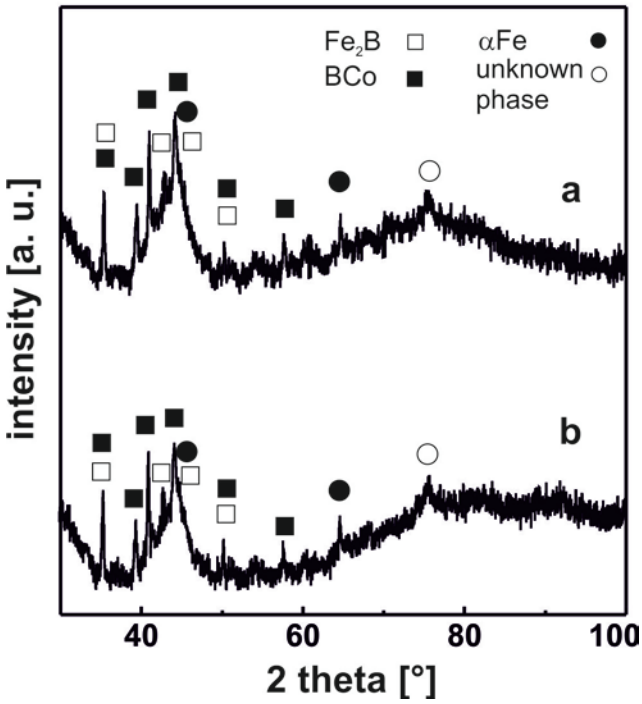

Figure 2. X-ray diffraction patterns for the alloy after solidification in powder form: (a) $Fe_{50}Co_{20}B_{20}Cu_1Nb_9$, (b) $Fe_{45}Co_{25}B_{20}Cu_1Nb_9$.

The diffractograms are typical for two-phase alloys consisting of an amorphous matrix and crystal grains distributed in its volume. Crystalline phases were identified using the Match program. Based on the diffractograms using the Sherrer formula, the average sizes of the resulting crystallites for particular phases were determined (Table 1).

Table 1. Estimated average crystallite sizes produced during rapid cooling of the liquid alloy $Fe_{50-x}Co_{20+x}B_{20}Cu_1Nb_9$.

Alloy \ Crystalline phase	Fe_2B [nm]	BCo [nm]	αFe [nm]
$Fe_{50}Co_{20}B_{20}Cu_1Nb_9$	30,2	23,2	15,6
$Fe_{45}Co_{25}B_{20}Cu_1Nb_9$	29,1	30,6	16,1

In the volume of the alloys, the share of the crystalline phases was identified, and the estimated average grain sizes for the individual phases are similar. It can be stated that the dynamics of the crystallization process in this case nucleation of crystal grains is similar for both alloys. This means that the process energy for the transformation of the second type is similar. Estimated mean grain sizes for all identified crystalline phases do not exceed the 100nm dimension, which allows to qualify the obtained samples as a nanocrystalline material [19]. During the solidification process, crystalline phases rich in iron, cobalt and boron were formed. As it is known, the presence of copper and niobium atoms in appropriate proportions affects the formation of fine-grained structure, which in turn has a significant impact on improving the magnetic properties of the material produced [20-23]. A small addition of copper made it possible to create a material with a nanocrystalline structure. Most likely the copper or niobium placed on the grain boundaries were small enough that their identification with XRD was impossible.

Samples of $Fe_{50-x}Co_{20+x}B_{20}Cu_1Nb_9$ in the form of powders were measured using magnetic weight In the fucntion of temperature using Faraday balance.

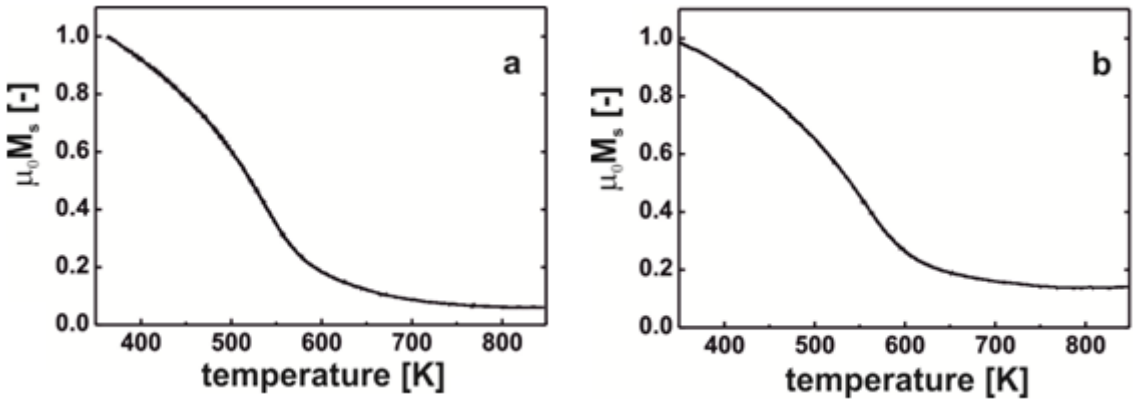

Figure 3. Magnetic polarization curves of saturation as a function of temperature: (a) $Fe_{50x}Co_{20}B_{20}Cu_1Nb_9$, (b) $Fe_{45}Co_{25}B_{20}Cu_1Nb_9$.

Figure 3 shows reduced magnetic saturation polarization curves. The measurement was carried out in the range from room temperature to 850K. In the examined range, one of the inflections from the transition of the amorphous phase from the ferro to the paramagnetic state is observed for the magnetization curves. As the temperature increases, the magnetization of the test sample decreases but does not drop to 0, which may be a confirmation of the presence of other magnetic phases occurring in the volume of the alloy (αFe, BCo, Fe_2B). The Curie temperature of these phases is outside the measurement range. The measured magnetic saturation polarization curves were subjected to numerical analysis. To determine the Curie temperature of the amorphous phase, a critical coefficient of 0.36 was used for ferromagnetics that met the Heisenberg assumptions. Curie temperature curves are shown in Figure 4.

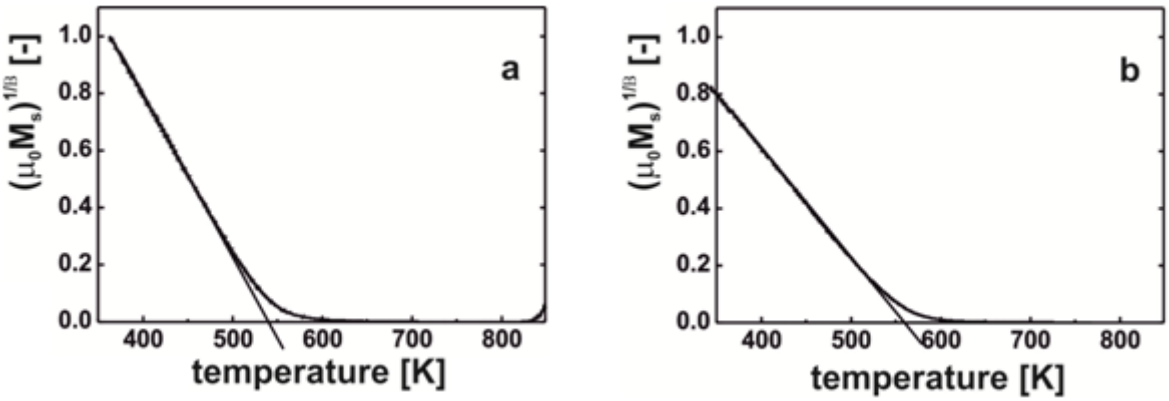

Figure 4. Dependence $\mu_0 M)^{1/\beta}(T)$ for alloys: a) $Fe_{50}Co_{20}B_{20}Cu_1Nb_9$, b) $Fe_{45}Co_{25}B_{20}Cu_1Nb_9$.

The Curie temperature for the $Fe_{50}Co_{20}B_{20}Cu_1Nb_9$ alloy is 540K while the $Fe_{45}Co_{25}B_{20}Cu_1Nb_9$ alloy is 557K. These results are in line with expectations, it is known that increasing the cobalt content in the alloy increases the Curie temperature value. However, the Curie temperature increase is small compared to increasing the cobalt content of the alloy at the expense of iron. In work [24], a 2% change in the cobalt content at the expense of iron raises the Curie temperature by 20K. Smaller than expected, the increase may be related to the larger average grain size of the cobalt rich phase (BCo) for the $Fe_{45}Co_{25}B_{20}Cu_1Nb_9$ alloy. It is possible to absorb more cobalt to the crystalline phase BCo in

the case of $Fe_{45}Co_{25}B_{20}Cu_1Nb_9$ alloy, which may be a reason for reducing the content of these elements in the amorphous matrix. Therefore, a slight increase in Curie temperature may be observed depending on the cobalt content in the alloy. It should be remembered that for amorphous materials, the Curie temperature is not a discrete value but rather a temperature range in which the amorphous matrix passes from the ferro-to-paramagnetic phase. This fact is closely related to the structure of the amorphous structure. The volume of amorphous material contains areas of similar chemical composition, which is not the case with the crystalline state. These small differences affect local differences in the Curie temperature value, therefore the value determined is not a discrete value.

Figure 5 contains static magnetic hysteresis loops. The measurement was made with the LakeShore vibration magnetometer in the magnetic field up to 2T.

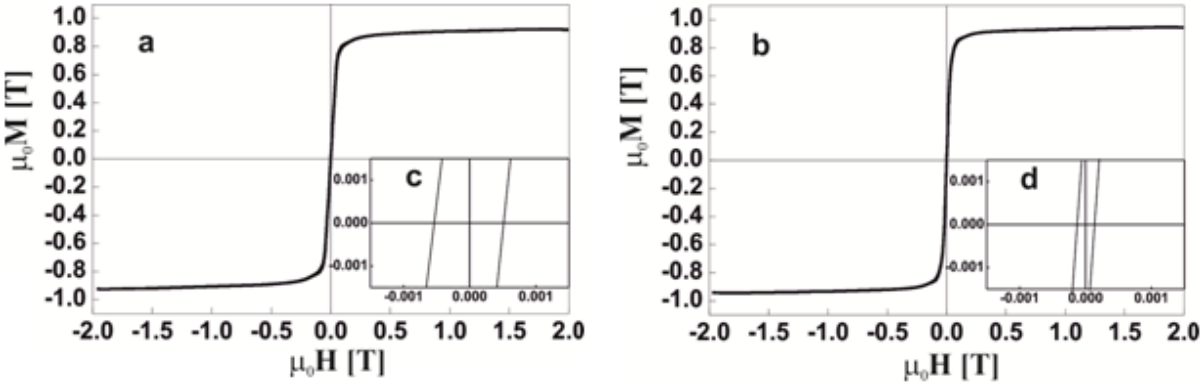

Figure 5. Static hysteresis loops with zoom in the center of M-H for: (a) and c) $Fe_{50}Co_{20}B_{20}Cu_1Nb_9$, (b) and d) $Fe_{45}Co_{25}B_{20}Cu_1Nb_9$.

The shape of static magnetic hysteresis loops indicates the magnetically soft properties. The shape of the wasp-like is not observed in the recorded loops, which excludes the presence of magnetic hard and semi-hard phases in the samples. The saturation magnetitization for the $Fe_{50}Co_{20}B_{20}Cu_1Nb_9$ alloy is 0.92T, while the value of the coercive field read from the enlarged coordinate system is 98A/m. For $Fe_{45}Co_{25}B_{20}Cu_1Nb_9$ alloy saturation magnetization equal to 0.95T and coercive field value 418A/m were measured. The measured saturation magnetization values can be considered relatively high. The coercive field values hold the created alloys in the group of so-called soft magnetic materials, assuming that these materials have a coercive field value below 1000A / m [25-26].

4. Conclusions

The purpose of the work was to create a material with soft magnetic properties by the method of rapid cooling of a liquid alloy. A volumetric rapid-cooled alloy was produced. The pressing method was used for this. The studies carried out allow to draw the following conclusions:

It is possible to produce a nanocrystalline material in a one-step manufacturing process, i.e. without heat treatment of the material. The impact on the formation of grains of crystalline phases not exceeding the size of 100nm is possible by introducing appropriate proportions of elements forming nucleation centers and inhibiting the crystallization process, copper and niobium.

The cooling rate of 10^2 K / s is sufficient to produce a nanocrystalline structure in the volume of the alloy with the chemical composition $Fe_{50-x}Co_{20+x}B_{20}Cu_1Nb_9$ (where x = 0, 5). FeCoB based rapid cooled alloys are characterized by a relatively high Curie temperature value, and the effect of cobalt content on the increase in Curie temperature is confirmed.

The increase in the cobalt content at the expense of iron in the tested alloy affects a slight decrease in the saturation magnetization value with a significant decrease in the coercive field value.

5. References

[1] Klement W, Willens R H, Duwez P 1960 *Nature* **187** 869-870
[2] Nabiałek M 2016 *Arch. Metall. Mater*. **61** 439–444
[3] Inoue A, Yano N, Masumoto T 1984 *J. Mater. Science* **19** 3786-3795
[4] Chen H S, Miller C E 1970 *Review of Scientific Instruments* **41** 1237
[5] Mchenry M E, Willard M A, Laughlin D E 1999 *Prog. Mater. Sci.* **44** 291
[6] Gruszka K *Materiali in Tehnologije* **50(5)** 707-718
[7] Błoch K, Nabiałek M 2015 *Acta. Phys. Pol. A* **127** 442–444
[8] Inoue A, Kato A, Zhang T, Kim S G, Masumoto T 1991 *Materials Transaction JIM* **32** 609-616
[9] Yanai T, Yamasaki M, Nakano M, Fukunaga H, Yoshizawa Y 2003 *Soft Magnetic Materials* **10** 737-741
[10] Herzer G 2013 *Acta Mater* **61** 718
[11] Błoch K 2015 *J. Magn. Magn. Mater*. **390** 118–122
[12] Jeż B, Nabialek M, Pietrusiewicz P, Gruszka K, Błoch K, Gondro J, Rzącki J, Abdullah M M A B, Sandu A V, Szota M, Jeż K, Sałagacki A 2017 *IOP Conf. Series: Materials Science and Engineering* **209** 012023
[13] Roy R K, Panda A K, Mitra A 2016 *Journal of Magnetism and Magnetic Materials* **418** 236–241
[14] Zhang Y,Wang Y, Makino A 2018 *Aip Advances* **8** 047703
[15] Herze G 1995 *Scripta Metallurgica et Materialia* **33** 1741-1756
[16] Han Y, Wang Z, Xu Y, Xie Z, Li L 2016 *Journal of Non-Crystalline Solids* **442** 29–33
[17] Wang W H, Dong C H 2004 *Materials Science and Engineering R* **44** 45-89
[18] Li W, Yang Y Z, Xu J 2017 *Journal of Non-Crystalline Solids* **461** 93–97
[19] Leonowicz M 1998 *Nanokrystaliczne materiały magnetyczne*, Warszawa
[20] Yoshizawa Y, Fujii S, Ping D H, Ohnuma M, Hono K 2003 *Scripta Mater* **48** 863
[21] Hono K, Ping D H, Ohnuma M, Onodera H 1999 *Acta Mater* **47** 997
[22] Pradeep K G, Herzer G, Choi P, Raab D 2014 *Acta Materialia* **68** 295-309
[23] Hono K, Inoue A, Sakurai T 1991 *Apel. Phys. Lett*. **58(19)** 2180-2182
[24] Jeż B 2017 *Revista de Chimie* **68(8)** 1903-1907
[25] Liebermann H 1993 *Rapidly Solidified Alloys* New Jersey